1 **The grape powdery mildew resistance loci *Ren2, Ren3, Ren4D,***

2 ***Ren4U, Run1, Run1.2b, Run2.1,* and *Run2.2* activate different**

3 **transcriptional responses to *Erysiphe necator***

4

5 Mélanie Massonnet[1], Summaira Riaz[1], Dániel Pap[1], Rosa Figueroa-Balderas[1], M. Andrew

6 Walker[1], Dario Cantu[1*]

7 [1]Department of Viticulture and Enology, University of California Davis, Davis, CA, United States

8

9 [*]**Correspondence:** dacantu@ucdavis.edu

10

11 **Running title:** Functional diversity of R loci in grapes

12

13 **Keywords**: Grape, powdery mildew, genetic disease resistance, disease evaluation, comparative

14 transcriptomics

15

Abstract

Multiple grape powdery mildew (PM) genetic resistance (*R*) loci have been found in wild grape species. Little is known about the defense responses associated with each *R* locus. In this study, we compare the defense mechanisms associated with PM resistance in interspecific crosses segregating for a single *R* locus from *Muscadinia rotundifolia* (*Run1*, *Run1.2b*, *Run2.1*, *Run2.2*), *Vitis cinerea* (*Ren2*), *V. romanetii* (*Ren4D* and *Ren4U*), and the interspecific hybrid Villard blanc (*Ren3*). By combining optical microscopy, visual scoring, and biomass estimation, we show that the eight *R* loci confer resistance by limiting infection at different stages. We assessed the defense mechanisms triggered in response to PM at 1 and 5 days post inoculation (dpi) via RNA sequencing. To account for the genetic differences between species, we developed for each accession a diploid synthetic reference transcriptome by incorporating into the PN40024 reference homozygous and heterozygous sequence variants and *de novo* assembled transcripts. Most of the *R* loci exhibited a higher number of differentially expressed genes (DEGs) associated with PM resistance at 1 dpi compared to 5 dpi, suggesting that PM resistance is mostly associated with an early transcriptional reprogramming. Comparison of the PM resistance-associated DEGs showed a limited overlap between pairs of *R* loci, and nearly half of the DEGs were specific to a single *R* locus. The largest overlap of PM resistance-associated DEGs was found between *Ren3$^+$*, *Ren4D$^+$*, and *Ren4U$^+$* genotypes at 1 dpi, and between *Ren4U$^+$* and *Run1$^+$* accessions at 5 dpi. The *Ren3$^+$*, *Ren4D$^+$*, and *Ren4U$^+$* were also found to have the highest number of *R* locus-specific DEGs in response to PM. Both shared and *R* locus-specific DEGs included genes from different defense-related categories, indicating that the presence of *E. necator* triggered distinct transcriptional responses in the eight *R* loci.

Introduction

Most cultivated grapevines (*Vitis vinifera* ssp. *vinifera*) are highly susceptible to powdery mildew (PM), a disease caused by the ascomycete *Erysiphe necator* Schwein (syn. *Uncinula necator*). *Erysiphe necator* is an obligate biotrophic pathogen that can infect any green tissue of the host. PM infections lead to reduced yield, and impaired fruit composition and wine quality (Calonnec *et al*., 2004; Stummer *et al*., 2005). Genetic resistance to PM has been found in several wild grapes, such as the North American grapes *Muscadinia rotundifolia* and *Vitis cinerea*, the Chinese *Vitis* species *V. piasezkii*, *V. romanetii*, *V. quinquangularis* and *V. pseudoreticulata*, and some Central Asian accessions of *V. vinifera* ssp. *sylvestris* (Dry *et al*., 2019). So far, thirteen PM resistance (*R*) loci have been genetically mapped (Dry *et al*., 2019; Karn *et al*., 2021) and named *Resistance to Uncinula necator* (*Run*) or *Resistance to Erysiphe necator* (*Ren*). Different allelic forms have been found for some of *Run* and *Ren* loci (Dry *et al*., 2019; Massonnet *et al*., 2022).

For most PM-resistant grape accessions, resistance to *E. necator* is associated with a programmed cell death (PCD)-mediated response (Qiu *et al*., 2015; Dry *et al*., 2019). Because PCD occurs in epidermal cells post-penetration of *E. necator*, the recognition of *E. necator*'s effectors by intracellular nucleotide-binding leucine-rich repeat (NLR) proteins is likely the trigger of PCD (Qiu *et al*., 2015; Dry *et al*., 2019). Only one NLR gene associated with PM resistance, *MrRUN1*, has been characterized in *M. rotundifolia* G52 (Feechan *et al*., 2013) and candidate NLR genes associated with *Run1.2b* and *Run2.2* have been proposed for *M. rotundifolia* Trayshed (Massonnet *et al*., 2022).

In plants, NLR activation leads to multiple cellular responses, such as the generation of reactive oxygen species (ROS), calcium oscillations, kinase activation, and an extensive transcriptional reprogramming resulting in the activation of defense-related mechanisms, including the biosynthesis of pathogenesis-related (PR) proteins and antimicrobial compounds, and cell wall modifications (Dangl *et al*., 2013; Lolle *et al*., 2020). NLR-triggered immunity generally involves PCD at the site of infection, which inhibits the development of the pathogen (Dangl *et al*., 2013; Lolle *et al*., 2020). In grapes, few studies have investigated the transcriptomic responses to *E. necator* infection in PM-resistant accessions (Amrine *et al*., 2015; Jiao *et al*., 2021; Weng *et al*., 2014). For example, comparative transcriptomics revealed that *E. necator* infection leads to diverse whole-genome transcriptional responses among Central Asian *V. vinifera* accessions

68   carrying different allelic forms of the *Ren1* locus (Amrine *et al*., 2015). Whether the resistance

69   conferred by different *R* loci depends on the activation of the same or different defense responses

70   is still an open question. Understanding the functional differences and overlap between *R* loci will

71   help select the most functionally diverse *R* loci to develop new *V. vinifera* cultivars that combine

72   durable resistance to PM and high-quality fruit production (Michelmore *et al*., 2013). However,

73   comparing genome-wide transcriptional changes in response to PM between *R* loci from different

74   *Vitis* species is challenging. Comparative transcriptomics using RNA sequencing (RNA-seq) data

75   relies on a reference transcriptome to evaluate transcript abundance. Recent studies showed that

76   grape genomes are highly heterozygous and substantially differ between *Vitis* species (Zhou *et al*.,

77   2019; Liang *et al*., 2019; Cochetel *et al*., 2021; Minio *et al*., 2022). A single haploid reference

78   transcriptome from a PM-susceptible *V. vinifera* biases the alignment of the RNA-seq reads,

79   underestimating the expression of alleles that are less similar to the reference, and confounding the

80   subsequent testing of differential gene expression.

81   In this study, we aimed to identify the defense mechanisms associated with eight *R* loci (*Ren2*,

82   *Ren3*, *Ren4D*, *Ren4U*, *Run1*, *Run1.2b*, *Run2.1*, and *Run2.2*) and to evaluate the functional

83   differences and overlap between them. First, we monitored PM disease development on leaves of

84   eight PM-resistant breeding lines, each representing a genetic *R* locus, as well as four PM-

85   susceptible sib lines and two PM-susceptible *V. vinifera* parents. Defense mechanisms associated

86   with each *R* locus were then assessed by profiling the leaf transcriptome with or without *E. necator*

87   inoculations. To enable the comparison of the transcriptional modulation in response to PM, we

88   constructed comparable reference transcriptomes incorporating both sequence variant information

89   into the reference transcriptome of PN40024 and *de novo* assembled transcripts. We also refined

90   the functional annotation of PN40024 predicted proteome to focus our analysis on genes involved

91   in defense mechanisms. Defense-related genes differentially expressed in response to the pathogen

92   were first compared between PM-resistant and PM-susceptible accessions to identify the genes

93   with a transcriptional modulation associated with PM resistance. The latter ones were then

94   compared between PM-resistant genotypes to evaluate the functional overlap between the different

95   *R* loci.

96

Materials and Methods

Plant material and evaluation of PM development

Fourteen grape accessions were used in this study: eight carrying one *R* locus, six sib lines without any *R* locus, and two susceptible *V. vinifera* parents. Information about the pedigree of each accession is provided in **Supplementary Table 1**.

PM susceptibility was evaluated with a detached leaf assay as described in Pap *et al*. (2016). Detached leaves were stained with Coomassie Brilliant Blue R-250 at 5 days post inoculation (dpi) as in Riaz *et al.* (2013). Visual disease susceptibility scores at 14 dpi were compared using a Kruskal-Wallis test followed by a post hoc Dunn's test ($P \leq 0.05$).

For transcriptional profiling, we followed the inoculation protocol described in Amrine *et al*. (2015). For each accession three plants were inoculated with *E. necator* C-strain (Jones et al., 2014) and three plants were mock-inoculated. Two leaves from each plant were collected 1 and 5 dpi and immediately frozen in liquid nitrogen. Leaves from an individual plant were pooled together and constitute a biological replicate. Three biological replications were obtained for each treatment.

RNA extraction, library preparation, and sequencing

RNA extraction and library preparation were performed as in Amrine *et al*. (2015). cDNA libraries were sequenced using Illumina HiSeq2500 and HiSeq4000 sequencers (DNA Technologies Core, University of California, Davis, CA, USA) as 50-bp single-end reads (**Supplementary Table 2**). Sequencing reads of the accessions e6-23 (*Run1.2b*[+]) and 08391-29 (*Run2.2*[+]) were retrieved from the NCBI BioProject PRJNA780568.

Reconstruction of accession-specific reference transcriptomes

For each accession, we constructed a reference transcriptome composed of a diploid synthetic transcriptome and *de novo* assembled transcripts. The diploid synthetic transcriptome was reconstructed using sequence variant information. First, adapter sequences were removed and RNA-seq reads were filtered based on their quality using Trimmomatic v.0.36 (Bolger *et al*., 2014) and these settings: LEADING:3 TRAILING:3 SLIDINGWINDOW:10:20 MINLEN:20. Quality-trimmed reads of the 12 samples from each accession were concatenated into a single file and

125   mapped onto a combined reference genome composed of *V. vinifera* PN40024 V1 (Jaillon *et al.*,

126   2007) and *E. necator* C-strain genome (Jones *et al.*, 2014) following the STAR 2-pass mapping

127   protocol (v.2.5.3a; Dobin *et al.*, 2013; Engström *et al.*, 2013). PCR and optical duplicates were

128   removed with Picard tools (v.2.0.1 http://broadinstitute.github.io/picard/), and reads were split into

129   exon segments using SplitNCigarReads from GATK v.3.5-0-g36282e4 (McKenna *et al.*, 2010).

130   GATK HaplotypeCaller was used to call sequence variants with the following parameters: -ploidy

131   2 -stand_call_conf 20.0 -stand_emit_conf 20.0 -dontUseSoftClippedBases. Variants were filtered

132   using GATK VariantFiltration with these settings: -window 35 -cluster 3 -filterName FS -filter

133   "FS > 30.0" -filterName QD -filter "QD < 2.0". Variants passing all filters were selected using

134   GATK SelectVariants with "--excludeFiltered" parameter. On average, $265,900 \pm 39,570$ variants

135   were detected per genotype (**Supplementary Table 3**). Variants in grape protein-coding regions

136   were extracted using bedtools intersect v.2.19.1 (Quinlan, 2014). Two separate genomes were

137   reconstructed for each genotype using the vcf-consensus tool from vcftools (Danecek *et al.*, 2011).

138   The first genome was reconstructed by incorporating both homozygous and heterozygous

139   alternative 1 (ALT1) variants relative to the PN40024 genome, while the second genome was

140   reconstructed using both homozygous and heterozygous alternative 2 (ALT2) variants. A new

141   annotation file was created for each genome from its corresponding variant information. CDS were

142   extracted using gffread from Cufflinks v.2.2.1 (Trapnell *et al.*, 2010).

143   For each genotype, quality-trimmed reads were mapped onto their respective diploid synthetic

144   grape transcriptome and *E. necator* C-strain CDS (Jones *et al.*, 2014) using Bowtie2 v.2.3.4.1

145   (Langmead and Salzberg, 2012) and the parameters --end-to-end --sensitive --un. For each grape

146   accession, *de novo* assembly was performed using unmapped reads from the 12 RNA-seq libraries

147   and TRINITY v.2.4.0 (Grabherr *et al.*, 2011). A total of 509,960 sequences were reconstructed,

148   corresponding to $36,426 \pm 2,585$ sequences per accession (**Supplementary Table 4**). To reduce

149   sequence redundancy, reconstructed transcripts from all 14 genotypes were clustered using CD-

150   HIT-EST v.4.6.8 (Li and Godzik, 2006) and an identity threshold of 90%. The longest

151   representative sequence of each of the 98,340 transcript clusters was used as input for

152   TransDecoder v.3.0.1 (https://github.com/TransDecoder/TransDecoder). For the 2,174 transcripts

153   with an open reading frame protein containing a start and a stop codon, the longest CDS was

154   selected. CDS redundancy was reduced by clustering using CD-HIT-EST v.4.6.8 (Li and Godzik,

155   2006), with coverage and identity thresholds of 100%. In total, 2,070 CDS were retained

156　(**Supplementary Data 1**). Taxonomic analysis of the predicted proteins was performed using

157　Megan v.6.12.5 (Huson *et al*., 2016) with default parameters after aligning predicted peptides

158　against the RefSeq protein database (ftp://ftp.ncbi.nlm.nih.gov/refseq, retrieved 17 January 2017).

159　The 103 peptides assigned to proteobacteria, opisthokonts, and viruses were considered microbial

160　contaminants; the remaining 1,967 peptides were assigned to grape (**Supplementary Table 5**).

161　To evaluate the effect of the reference transcriptome on the mapping rate (*i.e*. the percentage of

162　RNA-seq reads aligning onto the reference transcriptome), quality-trimmed RNA-seq reads were

163　aligned onto two reference transcriptomes: (i) the combined protein-coding sequences of *V.*

164　*vinifera* PN40024 V1 (Jaillon *et al*., 2007) and *E. necator* C-strain (Jones *et al*., 2014), (ii) the

165　combined accession-specific diploid synthetic grape transcriptome, the *de novo* assembled CDS,

166　and *E. necator* C-strain CDS (Jones *et al*., 2014), using Bowtie2 v.2.3.4.1 (Langmead and

167　Salzberg, 2012) and the parameters --end-to-end --sensitive --un. For each accession, the

168　difference of mapping rates between the two reference transcriptomes were tested using Kruskal-

169　Wallis test followed by post hoc Dunn's test ($P \leq 0.05$).

Gene expression analysis

171　Transcript abundance was assessed using Salmon v.1.5.1 (Patro *et al*., 2017) and these parameters:

172　--gcBias --seqBias --validateMappings. For each accession, a transcriptome index file was built

173　using the accession's diploid synthetic transcriptome combined with the *de novo* assembled

174　transcripts and the *E. necator* C-strain transcriptome, PN40024 V1 and *E. necator* C-strain

175　genomes as decoys, and a k-mer size of 13. Read counts were computed using the R package

176　tximport v.1.20.0 (Soneson *et al*., 2015). Read counts of the two haplotypes of each gene locus of

177　the diploid synthetic transcriptome were combined. Read-count normalization of the grape

178　transcripts and statistical testing of differential expression were performed using DESeq2 v.1.16.1

179　(Love *et al*., 2014). The sample 14305-001_H_5dpi_1 was removed from the RNA-seq analysis

180　because of its low mapping rate (**Supplementary Table 2**).

Functional annotation of the defense-related genes

182　To determine the defense mechanisms triggered by the presence of *E. necator*, we refined the

183　functional annotation of the grape predicted proteins involved in the following processes: pathogen

184　recognition by receptor-like kinases (RLKs) and intracellular receptors (NLRs), ROS production

185 and scavenging, nitric oxide (NO) production, calcium oscillations, MAPK cascade, salicylic acid

186 (SA), jasmonic acid (JA), ethylene (ET), and abscisic acid (ABA) signaling, pathogenesis-related

187 (PR) protein and phytoalexin biosynthesis, and cell wall reinforcement. Functional annotation of

188 the grape predicted proteins was assigned based on sequence homology with *Arabidopsis thaliana*

189 predicted proteins involved in the aforementioned functional categories and protein domain

190 composition. Grape proteins were aligned onto *A. thaliana* proteins

191 (Araport11_genes.201606.pep.fasta; https://www.arabidopsis.org/download/index.jsp) using

192 BLASTP v.2.6.0. Alignments with an identity greater than 30% and a reciprocal reference:query

193 coverage between 75% and 125% were kept. For each grape protein, the alignment with the highest

194 product of identity, query coverage, and reference coverage was selected to determine a

195 homologous protein in *A. thaliana*. We verified that each grape protein and its assigned *A. thaliana*

196 had a similar domain composition. Grape and *Arabidopsis thaliana* predicted proteins were

197 scanned with hmmsearch from HMMER v.3.3.1 (http://hmmer.org/) and the Pfam-A Hidden

198 Markov Models (HMM) database (El-Gebali *et al.*, 2019; downloaded on 29 January 2021).

199 Protein domains with an independent E-value less than 1.0 and an alignment covering at least 50%

200 of the HMM were selected. Grape predicted proteins having a similar domain composition than

201 their *A. thaliana* homologues were retained. The functional annotation of defense-related genes

202 used in this study can be found in **Supplementary Table 6**.

203

Results

Powdery mildew resistance loci exhibit different intensity and timing of response to *E.
necator*

207 PM disease severity was evaluated on detached leaves from fourteen grape accessions, including

208 twelve interspecific accessions, and two PM-susceptible *V. vinifera,* Malaga Rosada and F2-35

209 (**Table 1**, **Supplementary Table 1**). The twelve interspecific hybrids included four pairs of

210 siblings derived from backcrosses with one of the following resistant accessions: *V. romanetii*

211 C166-043 (*Ren4D*+), *V. romanetii* C166-026 (*Ren4U*+), *M. rotundifolia* G52 (*Run1*+), *M.*

212 *rotundifolia* Trayshed (*Run2.2*+) (Ramming *et al.*, 2011; Riaz *et al.*, 2011; Feechan *et al.*, 2013).

213 The four remaining interspecific accessions were 09390-023 (*Ren2*+), 07712-06 (*Ren3*+), e6-23

214 (*Run1.2b$^+$*), and 09705-45 (*Run2.1$^+$*); these inherited PM resistance from *V. cinerea* B9, the

215 interspecific hybrid Villard blanc, *M. rotundifolia* Trayshed, and *M. rotundifolia* Magnolia,

216 respectively (Dalbó e*t al.*, 2001; Riaz e*t al.*, 2011; Zyprian e*t al.*, 2016).

217

218 **Table 1**: Description of the fourteen grape genotypes used in this study. Details about their

219 pedigree are provided in **Supplementary Table 1**. Siblings deriving from the same cross are

220 indicated with an asterisk. BC, backcross.

Accession name	*R* locus	*R* locus origin	BC level	% *V. vinifera*
09390-023	*Ren2$^+$*	*V. cinerea* B9	F1	50
07712-06	*Ren3$^+$*	Villard blanc	Complex	78
13353-55*	*Ren4D$^+$*	*V. romanetii* C166-043	BC2	87.5
13353-33*	*Ren4D$^-$*	-	BC2	87.5
14305-002*	*Ren4U$^+$*	*V. romanetii* C166-026	Complex	89.1
14305-001*	*Ren4U$^-$*	-	Complex	89.1
14375-059*	*Run1$^+$*	*M. rotundifolia* G52	BC4	96.9
14375-063*	*Run1$^-$*	-	BC4	96.9
e6-23	*Run1.2b$^+$*	*M. rotundifolia* Trayshed	BC2	87.5
09705-45	*Run2.1$^+$*	*M. rotundifolia* Magnolia	BC2	87.5
08391-029*	*Run2.2$^+$*	*M. rotundifolia* Trayshed	BC3	93.8
08391-028*	*Run2.2$^-$*	-	BC3	93.8
F2-35	-	-	-	100
Malaga Rosada	-	-	-	100

221

222 At 5 dpi, extensive hyphal growth and conidiophores were observed on leaves from the two PM-

223 susceptible *V. vinifera* cultivars, F2-35 and Malaga Rosada, and all the sib lines devoid of PM

224 resistance loci (**Figure 1A**). Little or no hyphal growth was visible on the leaves of the accessions

225 carrying *Ren4D*, *Ren4U*, *Run1*, and *Run1.2b* loci. Some secondary and tertiary hyphae were found

226 on *Ren2$^+$*, *Ren3$^+$*, *Run2.1$^+$*, and *Run2.2$^+$* genotypes (**Figure 1A**). PM infection was also assessed at

227 an advanced disease development stage (14 dpi) using visual scoring (**Supplementary Figure**

228 **1A**). Infection rate at 5 and 14 dpi was similar for all genotypes except *Ren2$^+$* and *Ren3$^+$*, which

229   both had an extensive mycelium growth on their leaves at 14 dpi (Kruskal-Wallis test followed by

230   post-hoc Dunn's test; $P \leq 0.05$).

231   PM biomass on leaves was estimated by measuring *E. necator* transcript abundance at 5 dpi. As

232   expected, significantly lower *E. necator* transcript counts were found in genotypes carrying a PM

233   *R* locus (**Figure 1B,C**). Significant differences in *E. necator* transcripts were also observed

234   between *Ren2⁺*, *Run2.2⁺*, and the other PM-resistant accessions (Kruskal-Wallis test followed by

235   post hoc Dunn's test; $P \leq 0.05$). *E. necator* transcript abundance at 5 dpi and PM infection scores

236   at 14 dpi correlated well ($R^2 = 0.71$; **Supplementary Figure 1B**), which suggests that pathogen

237   transcript abundance is a reliable measure of PM susceptibility.

238   These results show that all *R* loci confer resistance to PM in *V. vinifera*. However, PM resistance

239   level varies between *R* loci, suggesting differences in the perception of the pathogen and/or in the

240   efficiency of the defense responses.

241
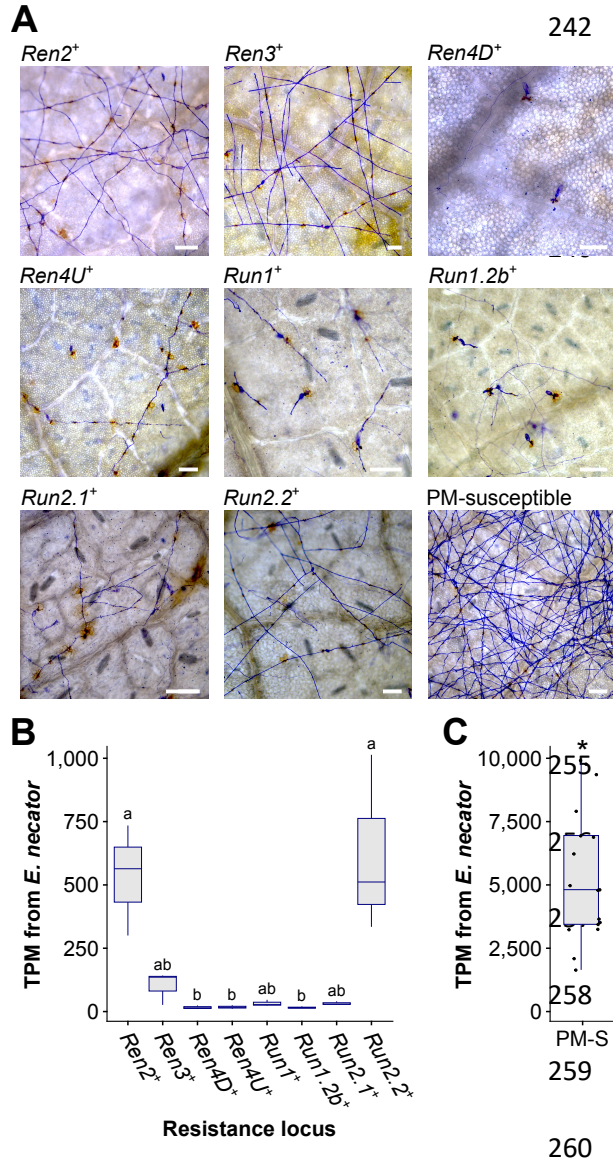
Figure 1: Powdery mildew disease development at 5 days post-inoculation. (**A**) Micrographs of detached leaves inoculated with *E. necator*. Scale = 100 μm. Total Transcripts per Million (TPM) derived from *E. necator* transcriptome in PM-resistant (**B**) and PM-susceptible (PM-S) accessions (**C**). Significant differences between PM resistance loci are indicated by different letters (Kruskal-Wallis test followed by post hoc Dunn's test; $P \leq 0.05$). Significant difference between grape accessions with and without a PM resistance locus is indicated by an asterisk (Kruskal-Wallis test, $P = 4.0 \times 10^{-8}$).

261

Construction of comparable reference transcriptomes

To determine if the differences in PM development between *R* loci were associated with differences in the defense mechanisms induced, we profiled the leaf transcriptomes of the fourteen genotypes at 1 and 5 dpi using RNA-seq. Mock-inoculated samples were collected as controls. Because the genotypes have diverse and distant genetic backgrounds, we built comparable reference transcriptomes for each genotype by incorporating sequence variant information into the

11

268 predicted transcriptome of PN40024 and by adding *de novo* assembled transcripts that are not
269 found among the annotated CDS of PN40024.

270 RNA-seq reads were first used to identify sequence polymorphisms between all sequenced
271 transcriptomes and the PN40024 reference (Jaillon *et al*., 2007). On average, $109,645 \pm 17,463$
272 single-nucleotide polymorphisms (SNPs) and $1,208 \pm 119$ short insertion-deletions (INDELs)
273 were detected in the protein-coding regions of each grape accession (**Figure 2**; **Supplementary**
274 **Table 3**). Although the number of homozygous SNPs was quite stable across genotypes (35,490
275 $\pm 4,667$), the number of heterozygous SNPs varied extensively, ranging from 54,154 in *V. vinifera*
276 cv. Malaga Rosada to 116,032 in the *Ren2*^{+} accession (Malaga Rosada x *V. cinerea* B9; **Figure 2**).
277 Comparison of the SNPs detected in the fourteen leaf transcriptomes compared to *V. vinifera*
278 PN40024 protein-coding sequences distinguished the *Ren2*^{+} accession from the other grape
279 accessions, likely because it is the only F1 individual in this study (**Table 1**; **Figure 2**). Siblings
280 and respective *V. vinifera* parents clustered together confirming the validity of the variant calling
281 approach (**Figure 2**). Analysis of genetic relatedness also confirmed sibling and parent-offspring
282 relationships (**Supplementary Figure 2**). Homozygous and heterozygous variants of each grape
283 genotype were incorporated into the CDS of PN40024 to produce a diploid reference transcriptome
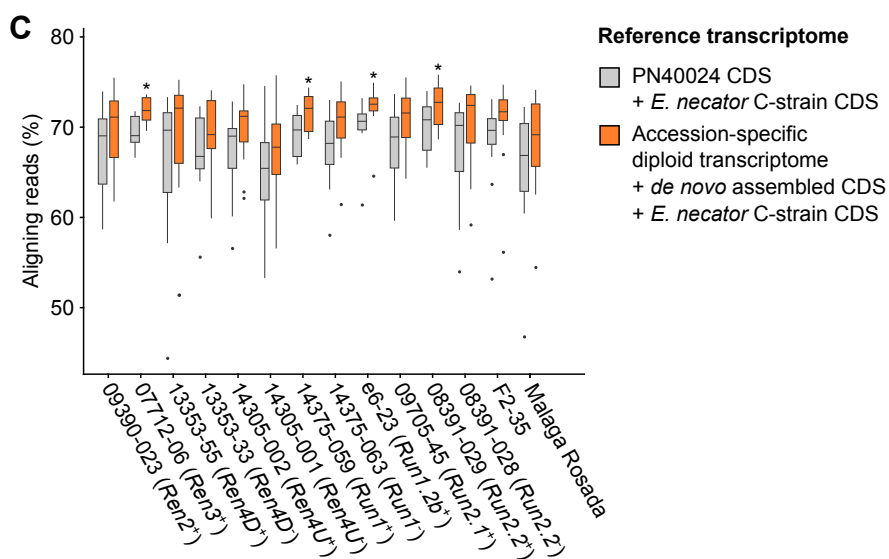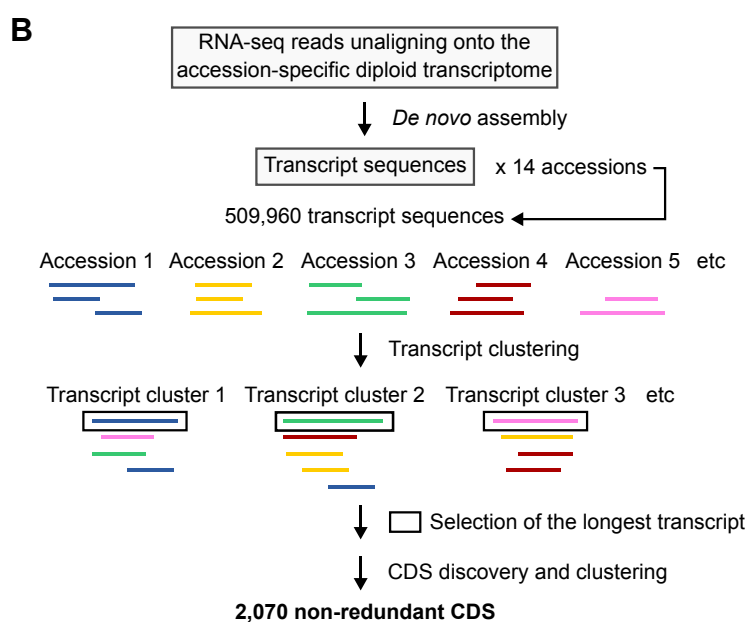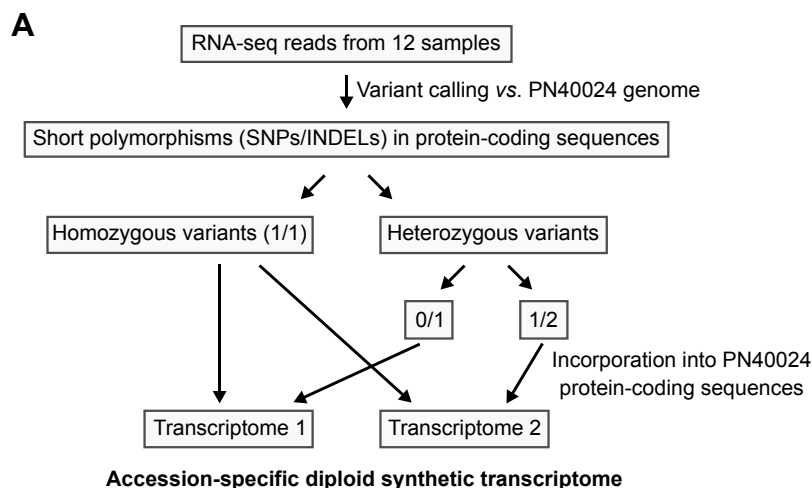284 for each genotype (**Figure 3A**).

285
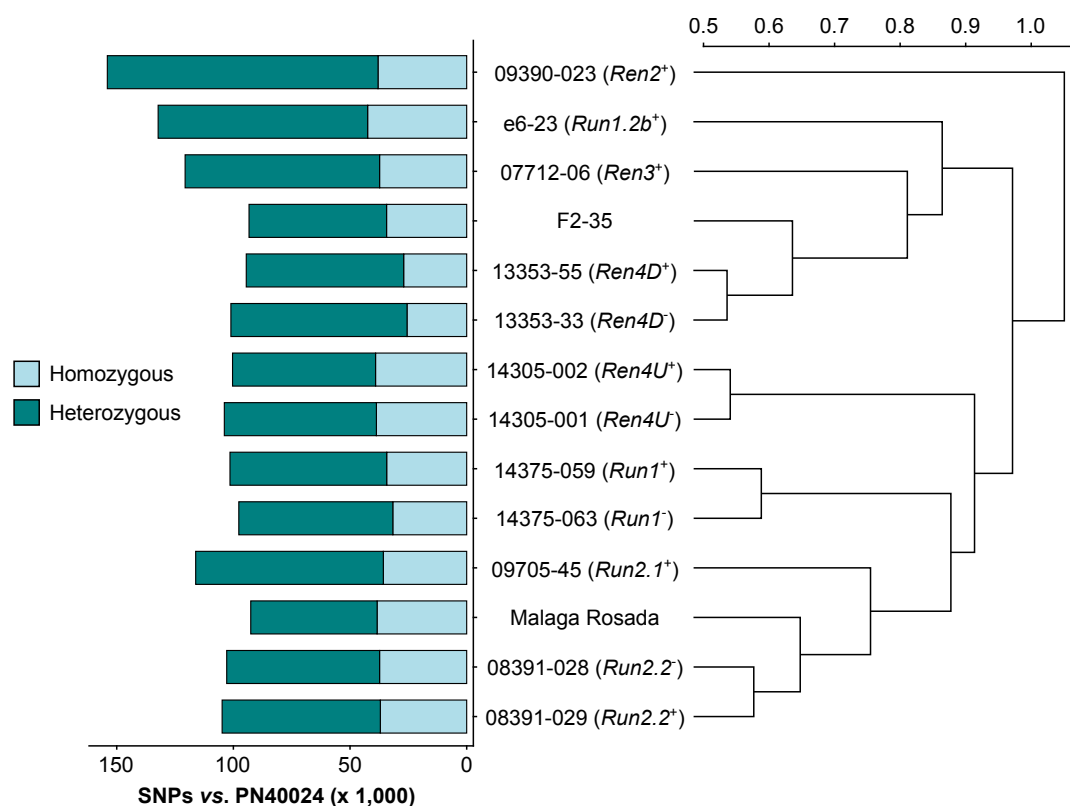
Figure 2: SNPs detected in the leaf transcriptome of the 14 grape accessions compared to the protein-coding sequences of *Vitis vinifera* PN40024. The Pearson correlation coefficients of the pairwise SNP comparison were converted into distance coefficients to define the height of the dendrogram branches.

The RNA-seq reads that did not align onto their respective diploid transcriptome reference were *de novo* assembled in order to construct transcripts that are not present in the PN40024 transcriptome (**Figure 3B**). All *de novo* assembled transcripts from the fourteen accessions were clustered to obtain a non-redundant dataset. After sequence clustering, CDS discovery, and removal of non-plant sequences, 1,967 non-redundant plant CDS were identified (See methods; **Supplementary Table 5**). Based on transcript clustering, each grape accession possessed on average $1,201 \pm 31$ of the grape *de novo* assembled CDS. As expected, siblings grouped together based on shared CDS (**Supplementary Figure 3**). Incorporating the sequence polymorphisms and *de novo* assembled CDS into the reference transcriptome increased the percentage of aligning

301 RNA-seq reads by $2.5 \pm 0.9\%$ per sample (**Figure 3C**) and likely also increased the mapping

302 specificity.

A

RNA-seq reads from 12 samples

↓ Variant calling *vs*. PN40024 genome

Short polymorphisms (SNPs/INDELs) in protein-coding sequences

Homozygous variants (1/1)   Heterozygous variants

0/1   1/2

Incorporation into PN40024 protein-coding sequences

Transcriptome 1   Transcriptome 2

Accession-specific diploid synthetic transcriptome

B

RNA-seq reads unaligning onto the accession-specific diploid transcriptome

↓ *De novo* assembly

Transcript sequences   x 14 accessions

509,960 transcript sequences

Accession 1 Accession 2 Accession 3 Accession 4 Accession 5 etc

↓ Transcript clustering

Transcript cluster 1 Transcript cluster 2 Transcript cluster 3 etc

↓ □ Selection of the longest transcript

↓ CDS discovery and clustering

2,070 non-redundant CDS

C

Aligning reads (%)

Reference transcriptome

☐ PN40024 CDS
+ *E. necator* C-strain CDS

☐ Accession-specific diploid transcriptome
+ *de novo* assembled CDS
+ *E. necator* C-strain CDS

x-axis labels:
09390-023 (Ren2⁺)
07712-06 (Ren3⁺)
13353-55 (Ren3⁺)
13353-33 (Ren4D⁺)
14305-002 (Ren4D⁺)
14305-001 (Ren4D⁻)
14375-001 (Ren4U⁺)
14375-059 (Ren4U⁻)
e6-23 (Run1⁺)
09705-45 (Run1,2b⁺)
08391-045 (Run2.1⁺)
08391-029 (Run2.2⁺)
08391-028 (Run2.2⁻)
F2-35 (Run2.2⁻)
Malaga Rosada

303

15

304 **Figure 3**: Adapting the grape transcriptome to each accession enhances the alignment of RNA-
305 seq reads. Schematic representations of the bioinformatics approaches used to reconstruct the
306 diploid synthetic transcriptome of each grapevine accession (**A**) and to cluster the *de novo*
307 assembled transcripts (**B**). (**C**) Effect of the reference transcriptome on the percentage of aligning
308 reads. For each genotype, difference of mapping rate with the combined transcriptomes of
309 PN40024 and *E. necator* was tested using a Kruskal-Wallis test. * indicates *P* value ≤ 0.05.

310

311 **Annotation of the grape defense-related genes**

312 To determine the defense mechanisms involved in the response to *E. necator*, we refined the
313 functional annotation of the grape predicted proteins based on protein domain composition and
314 homology with *Arabidopsis thaliana* predicted proteins. We identified 2,694 grape genes involved
315 in the following processes: pathogen recognition by receptor-like kinases (RLKs) and intracellular
316 receptors (NLRs), ROS production and scavenging, nitric oxide (NO) production, calcium
317 oscillations, MAPK cascade, salicylic acid (SA), jasmonic acid (JA), ethylene (ET), and abscisic
318 acid (ABA) signaling pathways, pathogenesis-related (PR) protein and phytoalexin biosynthesis,
319 and cell wall reinforcement (**Table 2**; **Supplementary Table 6**). These included 22 *de novo*
320 assembled CDS, including nine NLRs, a glutaredoxin, three pathogenesis-related (PR) protein 14-
321 like proteins, and three ethylene-responsive transcription factors (ERFs) (**Supplementary Table**
322 **6**).

323

324 **Table 2**: Number of defense-related genes identified among the predicted proteins of PN40024
325 CDS and the *de novo* assembled CDS. NLR, nucleotide-binding leucine-rich repeat protein.

Defense-related functional category	PN40024 CDS	*de novo* CDS	Total
Receptor-like kinases (RLKs)	450	1	451
Nucleotide-binding leucine-rich repeat proteins (NLRs)	309	9	318
Calcium signaling	109	0	109
MAPK signaling	83	0	83
Reactive oxygen species (ROS) production	106	0	106
Reactive oxygen species (ROS) scavenging	216	1	217
Nitric oxide (NO) production	8	0	8

16

Salicylic acid-mediated signaling pathway	26	0	26
Jasmonic acid-mediated signaling pathway	113	1	114
Ethylene-mediated signaling pathway	168	3	171
Abscisic acid-mediated signaling pathway	111	0	111
Pathogenesis-related (PR) proteins	374	3	377
Phytoalexin biosynthesis	339	1	340
Cell wall reinforcement	260	3	263
Total	2,672	22	2,694

326

Assessment of the transcriptional modulations associated with powdery mildew resistance

328 PM- and mock-inoculated leaf transcriptomes were compared at 1 and 5 dpi to identify the defense-
329 related genes that were differentially expressed in response to *E. necator* (**Figure 4**;
330 **Supplementary Table 7**). In the PM-resistant vines *Ren3+*, *Ren4D+*, *Ren4U+*, and *Run1.2b+*, up-
331 and down-regulated genes were more numerous at 1 dpi relative to 5 dpi, while only few
332 differentially expressed genes (DEGs) were detected in *Run2.1+* leaves. The opposite pattern was
333 observed in the *Run2.2+* accession as well as four of the five PM-susceptible plants. These results
334 suggest that disease resistance is mostly associated with an early transcriptional reprogramming.

335 To determine the transcriptional modulations associated with PM resistance, defense-related
336 DEGs in PM-resistant accessions were compared with the ones found in PM-susceptible
337 individuals at each time point. On average, 39.7 % ± 16.6 % of the up-regulated genes and 52.7 %
338 ± 19.0 % of the down-regulated genes detected in PM-resistant accessions were not found in PM-
339 susceptible plants (**Figure 4**). PM resistance-associated DEGs were more numerous at 1 dpi
340 compared to 5 dpi in all PM-resistant genotypes except the *Ren4U+* vine. This supports the
341 hypothesis that an early transcriptional reprogramming caused by the prompt perception of *E.*
342 *necator* by intracellular NLR is crucial for PM resistance. However, the PM-resistant accessions
343 exhibited different amounts of defense-related DEGs in response to *E. necator* at 1 dpi. The highest
344 number of up-regulated genes associated with disease resistance at 1 dpi was detected in *Ren3+*,
345 *Ren4D+*, and *Ren4U+* vines (199, 193, and 167 genes, respectively), while a lower number of up-
346 regulated genes was found in *Ren2+*, *Run1+*, *Run1.2b+*, *Run2.2+* leaves (93, 59, 70, and 42 genes,
347 respectively). The *Run2.1+* accession was the PM-resistant with the fewest up-regulated genes
348 associated with PM resistance, with only 7 and 14 genes at 1 and 5 dpi, respectively. Similar
349 patterns were observed for the down-regulated genes detected only in PM-resistant vines.

17

350

351
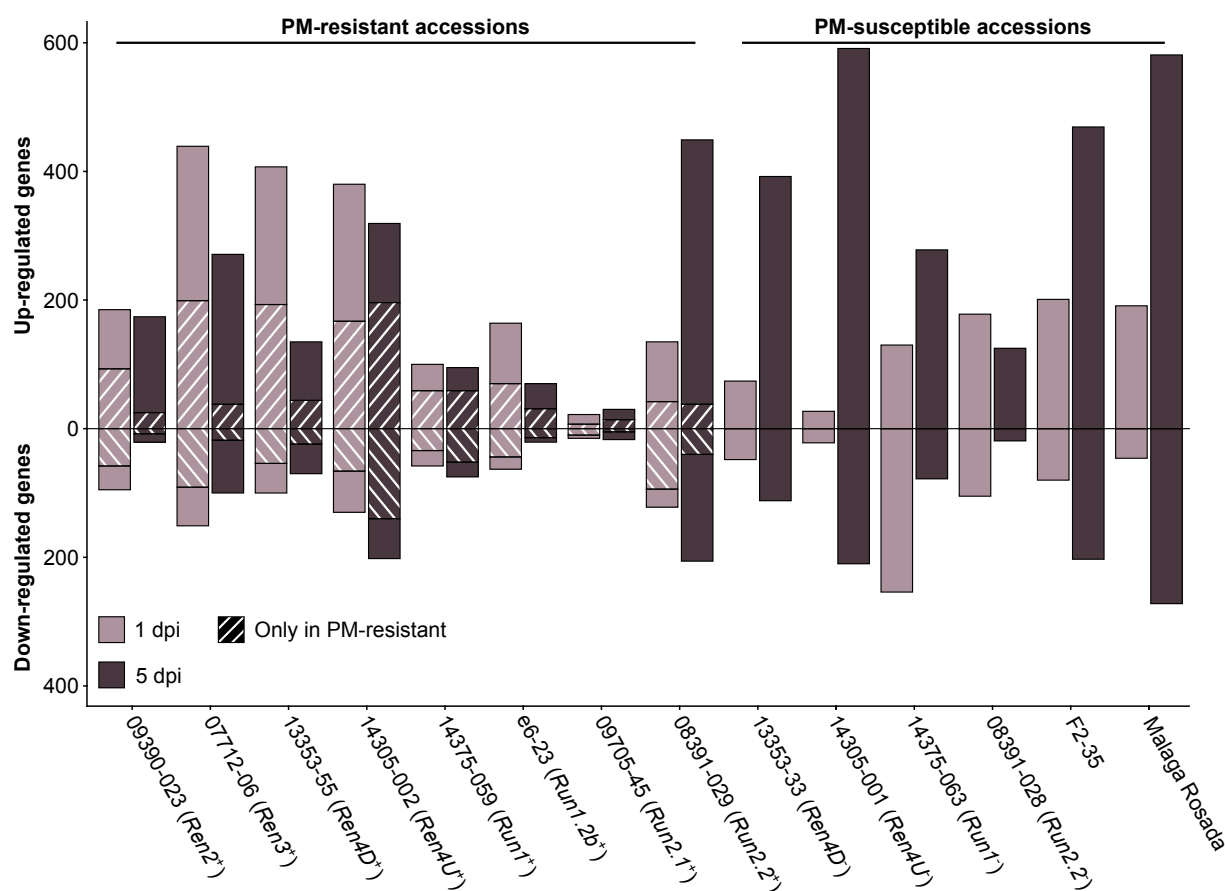
Figure 4: Defense-related genes differentially expressed in response to *E. necator* at 1 and 5 dpi. The genes uniquely differentially expressed by *E. necator* in the grape accessions possessing a *R* locus were identified by comparing the up- and down-regulated genes in PM-resistant leaves with the ones detected in PM-susceptible vines at each time point.

356

Overlap in transcriptional modulation associated with powdery mildew resistance between *R* loci

PM resistance-associated DEGs were compared across PM-resistant accessions to evaluate the overlap in defense responses between the different PM resistance loci (**Figure 5 & 6**; **Supplementary Figures 4-7**). On average, the *R* loci shared 52.9 ± 10.4 % and 38.0 ± 13.6 % of their defense-related DEGs associated with disease resistance with at least another *R* locus at 1 and 5 dpi, respectively. However, the overlap of PM resistance-associated DEGs between two *R* loci

18

364   was limited (8.4 ± 10.0 %). The largest pairwise overlaps were found among the up-regulated

365   genes at 1 dpi between the *Ren3⁺*, *Ren4D⁺*, and *Ren4U⁺* genotypes (**Figure 5A**, **Supplementary**

366   **Figure 4**). The *Ren3⁺* and *Ren4D⁺* accessions shared 64 up-regulated genes, while 49 and 44

367   defense-related genes were up-regulated in both *Ren3⁺* and *Ren4U⁺* genotypes, and both *Ren4D⁺*

368   and *Ren4U⁺* vines, respectively. The overlap of up-regulated genes between *Ren3⁺* and *Ren4D⁺*

369   accessions encompassed the largest number of extra- and intracellular receptor genes (15 RLK and

370   10 NLR genes), MAPK-signaling genes (7), and phytoalexin biosynthesis-related genes (11)

371   including six stilbene synthase genes (**Figure 5A**). Eight genes involved in ROS production were

372   found up-regulated in several *R* loci: a copper amine oxidase, three respiratory burst oxidase

373   homolog (RBOH), and four class III cell wall peroxidase (Prx) genes. Regarding ROS scavenging,

374   two catalase genes were up-regulated in both *Ren3⁺*, *Ren4D⁺*, and *Ren4U⁺* leaves, as well as seven

375   glutathione *S*-transferase genes in *Ren3⁺* and *Ren4U⁺* accessions. Some hormone-mediated

376   signaling genes were also found up-regulated genes in several *R* loci at 1 dpi, including one gene

377   involved in SA signaling, 12 genes in JA signaling, 13 genes in ET signaling, and 11 genes in

378   ABA signaling. The shared JA-signaling genes encompassed 8 genes involved in JA biosynthesis,

379   including an allene oxide synthetase (AOS) gene (VIT_18s0001g11630) that was more highly

380   expressed in *Ren3⁺*, *Ren4D⁺*, *Ren4U⁺*, *Run1.2b⁺* leaves in response to *E. necator*. The gene

381   *VviJAZ4* (VIT_09s0002g00890) encoding a jasmonate-ZIM-domain protein was also up-regulated

382   by the same PM resistance loci. Ectopic expression of *VqJAZ4* from *V. quinquangularis* was

383   showed to enhance resistance to PM in *A. thaliana*, suggesting a role of the jasmonate-ZIM-

384   domain protein in grape PM resistance (Zhang *et al*., 2019). Furthermore, *VviMYC2*

385   (VIT_02s0012g01320) was up-regulated in *Ren2⁺*, *Ren3⁺*, *Ren4D⁺*, and *Ren4U⁺* accessions at 1

386   dpi but not in any genotype possessing a *R* locus from *M. rotundifolia*. The same pattern was

387   observed for *VviJAR1* (VIT_15s0046g01280) which was up-regulated only in *Ren3⁺*, *Ren4D⁺*, and

388   *Ren4U⁺* accessions. In *A. thaliana*, JAR1 encodes a jasmonate-amido synthetase that catalyzes the

389   formation of the biologically active jasmonyl-isoleucine (JA-Ile) conjugate, while MYC2 is a basic

390   helix-loop-helix (bHLH) transcription factor that is involved in JA signaling but also in ABA- and

391   SA-mediated signaling (Abe *et al*., 2003; Dombrecht *et al*., 2007; Gautam *et al*., 2021; Staswick

392   and Tiryaki, 2004). Regarding cell wall reinforcement, a dirigent protein-encoding gene

393   (VIT_06s0004g01020) was up-regulated in *Ren4U⁺*, *Run1⁺* and *Run2.2⁺* genotypes at 1 dpi.

394   Dirigent proteins participate in the biosynthesis of lignans and lignin which both play a role in

395   plant defense. Lignans inhibit microbe-derived degradative enzymes while lignin accumulation in

396   the plant cell wall forms a physical barrier against pathogens (Paniagua *et al*., 2017). In addition,

397   the callose synthase genes *VviCalS1* and *VviCalS3* (Yu *et al*., 2016) were up-regulated in only

398   *Ren4D*^{+} and *Ren4U*^{+} accessions at 1 dpi and 5 dpi, respectively (**Figures 5A & 6A,**

399   **Supplementary Figures 4 & 6**). These results support previous observations which suggested that

400   *Ren4*-mediated resistance relies on the encasement of the pathogen haustorium in callose in

401   addition to PCD of the infected cells (Qiu *et al*., 2015).

402   Regarding the down-regulated genes associated with PM resistance at 1 dpi, *Ren3*^{+} and *Ren4U*^{+}

403   accessions shared the highest number of genes with a lower gene expression in response to *E.*

404   *necator* (20), followed by the *Ren2*^{+} and *Ren4D*^{+} vines (19), the *Run1.2b*[+] and *Run2.2*[+] plants (18),

405   and the *Ren4D*^{+} and *Ren4U*^{+} genotypes (17; **Figure 5B**). The overlap in down-regulated genes

406   between the *Ren3*^{+} and *Ren4U*^{+} accessions comprised 7 RLK genes, 2 Prx genes, and 2 cellulose

407   synthase-like genes. Both *Ren2*^{+} and *Ren4D*^{+} leaves exhibited a lower gene expression of 8 ROS

408   scavenging-related genes in response to *E. necator* at 1 dpi. Four fatty acid desaturase genes

409   involved in JA biosynthesis were down-regulated in the *Ren4D*^{+} and *Ren4U*^{+} genotypes, and an

410   ERF gene was down-regulated in *Ren3*^{+}, *Ren4D*^{+} and *Ren4U*^{+} plants.

411   At 5 dpi, the highest overlap of DEGs associated with PM resistance was found between *Ren4U*^{+}

412   and *Run1*^{+} genotypes, with 31 and 25 common up- and down-regulated genes, respectively (**Figure**

413   **6**). The shared up-regulated genes between *Ren4U*^{+} and *Run1*^{+} accessions encompassed 5 RLKs

414   and 17 NLRs, 3 MAPKK genes, 3 genes involved in ABA signal transduction, and the gene

415   encoding the exoribonuclease 4 (XRN4/EIN5; VIT_14s0030g01580) involved in ethylene

416   response (**Figure 6A**). Five additional ethylene-signaling genes were found up-regulated in *Ren2*^{+}

417   and *Ren4D*^{+} accessions at 5 dpi: a 1-aminocyclopropane-1-carboxylate synthase (ACS) gene

418   (VIT_02s0025g00360) and four ERF genes. In contrast, the 25 down-regulated genes shared by

419   *Ren4U*^{+} and *Run1*^{+} genotypes included six genes associated with ROS production (1) and

420   scavenging (6), and 10 genes involved in the biosynthesis of anthocyanins and condensed tannins
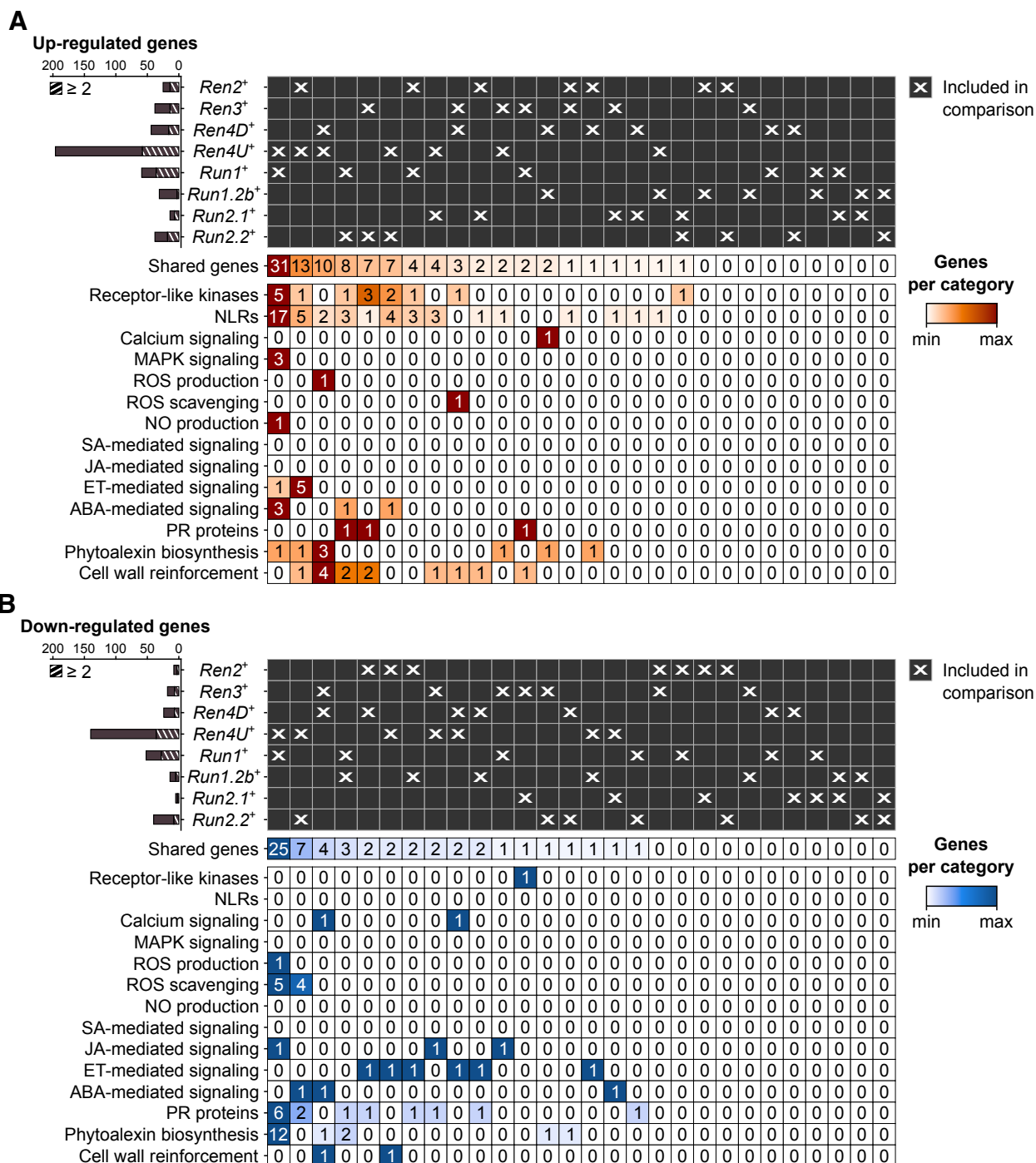
421   (**Figure 6B**).

422
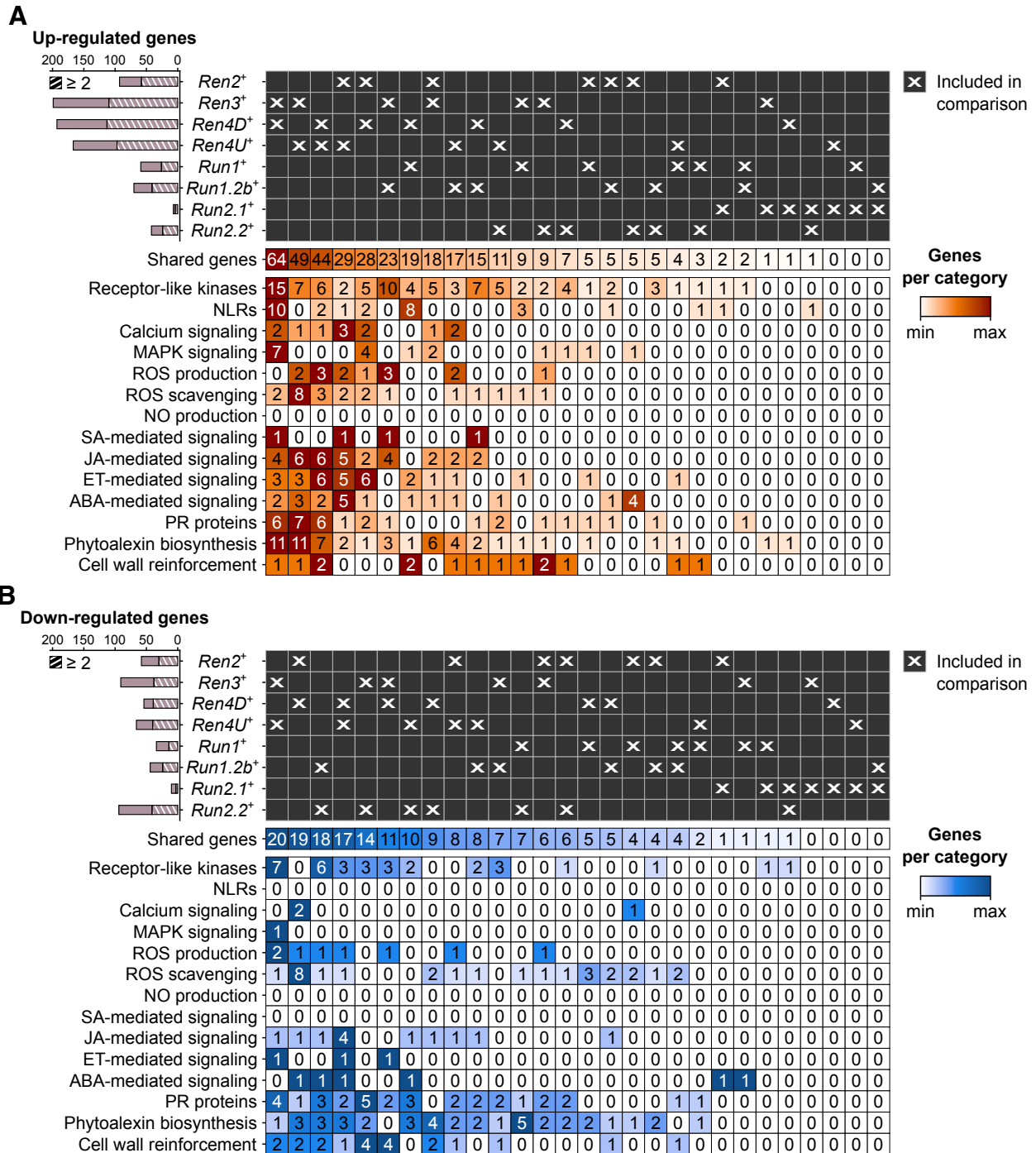
Figure 5: Pairwise comparison of the defense-related genes found up- and down-regulated in response to *E. necator* at 1 dpi in only the eight *R* loci. Striped bar plots depict the number of defense-related genes differentially expressed in at least two *R* loci.

21

Figure 6: Pairwise comparison of the defense-associated genes found up- and down-regulated in response to *E. necator* at 5 dpi in only the eight accessions carrying a *R* locus. Striped bar plots represent the defense-related genes differentially expressed in at least two *R* loci.

**Resistance locus-specific transcriptional modulations in response to *E. necator***

Nearly half of the PM resistance-associated DEGs were found in only one PM resistance locus (47.1 ± 10.4 % and 62.0 ± 13.6 % at 1 and 5 dpi, respectively). Although the *Ren3$^+$*, *Ren4D$^+$*, and *Ren4U$^+$* genotypes exhibited the greatest overlap of PM resistance-associated up-regulated genes at 1 dpi, the three PM resistance loci also had the highest number of genes (89, 80, and 70 genes, respectively) that were up-regulated in a *R* locus-specific manner (**Figure 7**). Regarding the down-regulated genes at 1 dpi, *Ren3$^+$* and *Run1.2b$^+$* plants had the most numerous *R* locus-specific ones (53 genes each). At 5 dpi, the largest number of *R* locus-specific DEGs was identified in *Ren4U$^+$* leaves, with 138 up-regulated and 104 down-regulated genes.

Differences in defense-related categories among the *R* locus-specific DEGs could be observed between the eight *R* loci and the two time points (**Figure 7**). The *Ren3$^+$* accession exhibited the greatest number of *R* locus-specific DEGs encoding intracellular receptors (RLKs) at 1 dpi, with 24 up-regulated and 19 down-regulated genes. In contrast, the presence of *E. necator* led to the up-regulation of 28 RLK and 44 NLR genes in only the *Ren4U$^+$* leaves at 5 dpi. In addition to the intra- and extracellular receptors, the *R* locus-specific DEGs encompassed several PR protein genes as well as genes involved in phytoalexin biosynthesis and cell wall rearrangement. Regarding the PR protein genes, the *Ren4U$^+$* accession showed the largest number of up-regulated genes at 1 dpi (11) but also the most numerous down-regulated genes at 5 dpi (28). The *Ren3$^+$* genotype had also some *R* locus-specific DEGs encoding PR proteins at 1 dpi (7 up-regulated and 9 down-regulated genes), while the *Ren4D$^+$* and *Run1.2b$^+$* vines had six and five specific up-regulated ones at 5 dpi, respectively. The PM resistance locus-specific DEGs encoding PR proteins included PR1-like proteins, beta-1,3-glucanases (PR2), basic chitinases (PR3), thaumatin-like proteins (PR5), subtilisin-like endoproteinases (PR7), chitinases type I (PR11) and III (PR8), Bet v 1 homologs (PR10), lipid-transfer proteins (PR14), and germin-like proteins (PR16). PM resistance loci also exhibited differences in *R* locus-specific DEGs involved in the biosynthesis of antimicrobial compounds. Like the PR proteins, the *Ren4U$^+$* accession had the highest number of genes that were up-regulated at 1 dpi (14) and down-regulated at 5 dpi (24) in a PM resistance locus-specific way. In addition to the *Ren4U$^+$* accession, several phytoalexin biosynthesis-related genes were found up-regulated only in the *Ren3$^+$*, *Ren4D$^+$*, and *Run1.2b$^+$* genotypes at both time points. In contrast, 21 genes involved in the biosynthesis of phytoalexins were found down-

463   regulated specifically in the *Run2.2*[+] plants at 1 dpi, including 18 genes from the phenylpropanoid

464   biosynthesis pathway. The *Ren3*^{+}-specific up-regulated genes at 1 dpi comprised three alkaloid-

465   related genes (berberine bridge enzymes), three genes from the phenylpropanoid biosynthesis

466   pathway: two cinnamate 4-hydroxylases (C4H) and one 4-coumarate--CoA ligase (4CL), and two

467   stilbene synthases. Genes involved in the biosynthesis of terpenoids and triterpenoids were also

468   found up-regulated in only one *R* locus at 1 dpi, such as two and three terpene synthase genes in

469   *Ren4D*^{+} and *Ren4U*^{+} accessions, respectively, as well as two and three oxidosqualene cyclase

470   genes in *Run2.2*[+] and *Ren4D*^{+} vines, respectively. Concerning the *R* locus-specific DEGs involved

471   in cell wall rearrangement, the *Ren4U*^{+} genotype had the largest number of both up- and down-

472   regulated genes. The *Ren4U*^{+}-specific up-regulated genes at 5 dpi included five cellulose synthase

473   genes, six cellulose synthase-like genes and two callose synthase genes: *VviCalS7*

474   (VIT_12s0028g00400) and *VviCalS10* (VIT_17s0000g10010). Another callose synthase gene,

475   *VviCalS11* (VIT_00s0265g00050), was also found up-regulated in *Run1*^{+} plants at 5 dpi. This

476   result suggests that *VviCalS11* could play a role in the accumulation of callose deposits described

477   in *Run1*^{+} plants (Feechan *et al*., 2015).

478
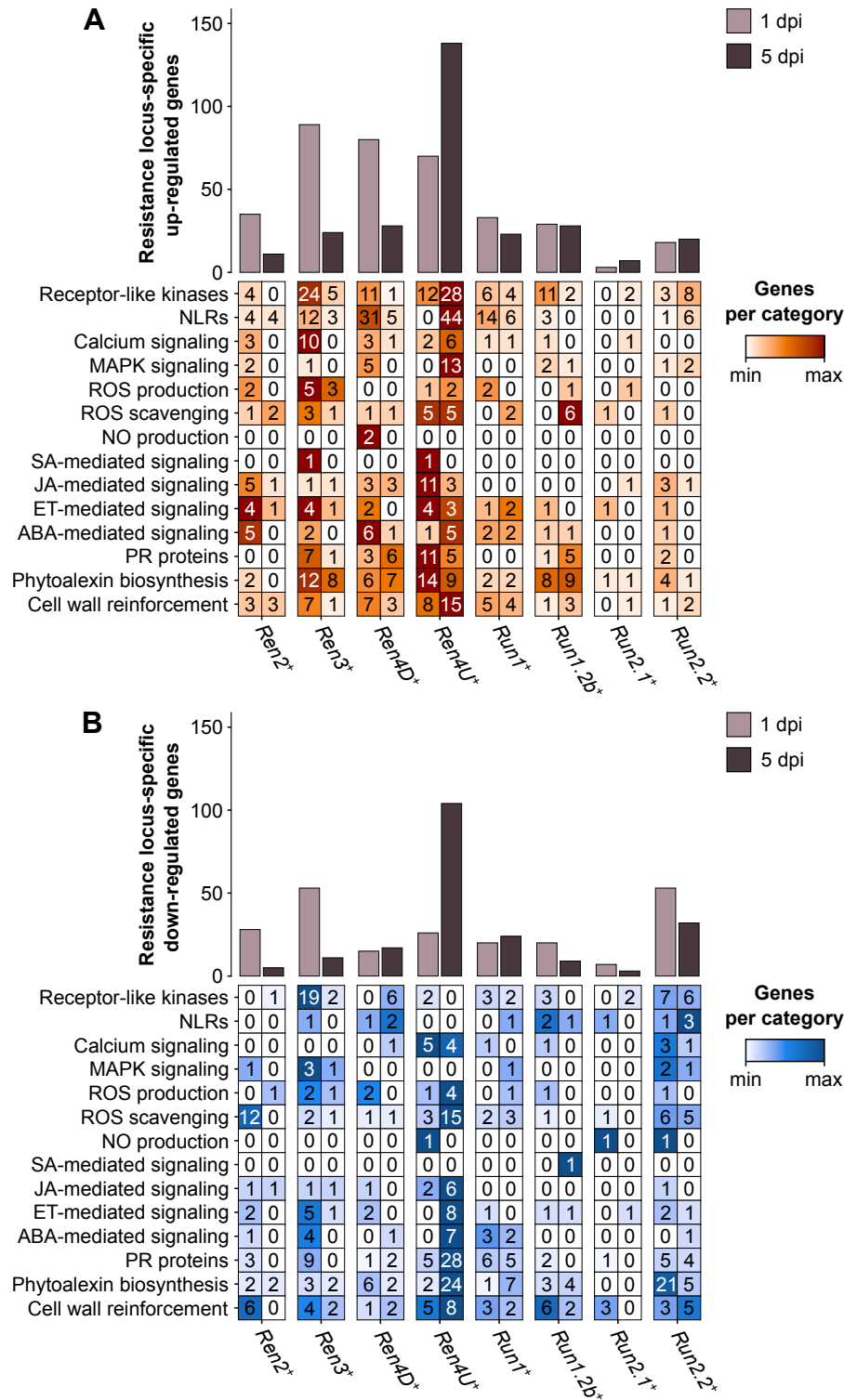
Figure 7: Defense-related categories among the genes identified as up-regulated (**A**) and down-regulated (**B**) by only one single PM resistance locus in response to *E. necator*.

Discussion

Powdery mildew resistance loci confer different levels of resistance to *E. necator*

Evaluation of PM development using microscopy, visual scoring, and total *E. necator* transcript abundance, revealed differences of intensity and timing of the response to *E. necator* at 5 and 14 dpi (**Figure 1**; **Supplementary Figure 1**). In particular, the *Ren2*, *Ren3* and *Run2.2* loci conferred a lower level of resistance to PM compared to the five other *R* loci. Similar disease phenotypes have been described for these *R* loci in previous studies (Qiu *et al*., 2015; Dry *et al*., 2019). The absence of primary hypha on the leaves of the *Ren4D$^+$*, *Ren4U$^+$*, *Run1$^+$*, and *Run1.2b$^+$* accessions and the very low transcript abundance for *E. necator* at 5 dpi suggest that restraint of the pathogen growth occurs rapidly in these vines, likely after haustorium formation at approximately 1 dpi (Leinhos *et al*., 1997). In contrast, the presence of some secondary and tertiary hyphae on *Ren2$^+$*, *Ren3$^+$*, *Run2.1$^+$*, and *Run2.2$^+$* genotypes' leaves suggest that restriction of *E. necator* happens at later time, between 1 and 2 dpi (Leinhos *et al*., 1997). In addition, fungal structures covered most of the leaves of *Ren2$^+$* and *Ren3$^+$* vines at 14 dpi, suggesting that these two *R* loci are less efficient in restricting the pathogen growth. Assessing the development of *E. necator* at additional time points post-inoculation and monitoring PCD would help to narrow down the difference of timing in the response to PM between the *R* loci. Furthermore, repeating the disease evaluation with additional breeding lines for each *R* locus would allow to confirm the observed phenotypes; while repeating the inoculation with additional *E. necator* isolates would help determine if the observed phenotypes are strain-specific.

Adapting the reference transcriptome allows comparing the transcriptional modulations of defense-related genes between different *Vitis* backgrounds

This study encompassed fourteen accessions with different genetic backgrounds making the comparison of the gene expression from orthologous genes challenging. To cope with this challenge, we incorporated small sequence polymorphisms (SNPs and INDELs) compared to the grape PN40024 CDS into a diploid synthetic transcriptome for each grape accession and performed a *de novo* assembly of the unaligned RNA-seq reads. The sequence variant analysis revealed an elevated number of heterozygous SNPs in the leaf transcriptomes of interspecific and intergeneric

512   hybrids compared to pure *V. vinifera* cultivars, reflecting the genetic diversity among *Vitis* species

513   and between *M. rotundifolia* and *Vitis* genera. The construction of the fourteen accession-specific

514   reference transcriptomes improved the alignment of the RNA-seq reads (**Figure 3C**). Complete

515   genome and/or transcriptome references of each grape accession would provide a more

516   comprehensive representation of the defense-related genes and potentially a more accurate

517   sequence for read alignment.

518   To assess the functional overlap among defense mechanisms between PM resistance loci, we

519   focused our study on the transcriptional modulation of 2,694 defense-related genes in response to

520   PM. These genes were selected based on functional domain composition and sequence similarity

521   with proteins of *A. thaliana*. Although the defense-related genes identified might not be exhaustive

522   and not definitive, the refinement of the functional annotation of PN40024 that was performed in

523   this study represents a valuable resource for the present and future transcriptomic studies of grape-

524   microbe interactions.

525

526   **Powdery mildew resistance loci trigger the transcriptional modulation of different defense-**

527   **related genes in response to *E. necator***

528   By comparing the transcriptomes of PM- and mock-inoculated leaves of eight PM-resistant and

529   six PM-susceptible grape accessions, we identified the defense-related DEGs associated with

530   disease resistance (**Figure 4**). Although the comparison of the PM resistance-associated DEGs

531   showed that the *R* loci shared DEGs to some extent, the overlap between two *R* loci was restricted

532   (8.4 ± 10.0 %). It is worth noting that no defense-related gene was found differentially expressed

533   in response to *E. necator* in more than five PM resistance loci (**Supplementary Figures 4-7**). In

534   addition, around half of the PM resistance-associated DEGs of each *R* locus was found specific

535   (**Figures 5 & 6**). Comparison of the *R* locus-specific DEGs showed that the eight *R* loci extensively

536   differ in their transcriptional response to *E. necator* through the transcriptional modulation of

537   specific defense-related genes (**Figure 7**). Interestingly, different allelic forms of the *Ren4*, *Run1*,

538   and *Run2* genetic loci exhibited different responses to *E. necator* and even shared a larger number

539   of DEGs with another genetic locus rather than with their respective haplotype (**Figures 5 & 6**).

27

540 To our knowledge, this study corresponds to the first attempt of comparing the transcriptional
541 modulations in response to PM between multiple *R* genetic loci. Previous studies focused on a
542 single *R* locus, a single PM-resistant accession (Fung *et al*., 2007; Jiao *et al*., 2021; Weng *et al*.,
543 2014), or multiple haplotypes of a single genetic locus (Amrine *et al*., 2015). Comparisons with
544 previous studies are difficult because different protocol of inoculation and different strains of *E.*
545 *necator* were used. Repeating the transcriptome profiling of additional recombinant lines for each
546 *R* locus, both PM-resistant and PM-susceptible, combined with whole-genome sequencing would
547 help dissect the *R* loci and identify the genes essential for resistance. Including other time points
548 may provide additional information to understand gene expression modulation earlier and later
549 than what considered in this study. For instance, few DEGs were detected for the $Run2.1^+$
550 accession, suggesting either that PM resistance is associated with the expression modulation of
551 few genes or that the transcriptional reprogramming in response to *E. necator* occurs at a different
552 time for the *Run2.1* locus.

553 Finally, this dataset represents a valuable resource for future breeding perspectives as it could help
554 select the most functionally diverse *R* loci to introgress into *V. vinifera*.

555

Data availability statement

557 RNA sequencing data are accessible through NCBI under the BioProject PRJNA897013.

558

Author contributions

560 D.C, M.A.W, S.R, and M.M. designed the project. S.R and D.P performed the sample inoculation,
561 collection, microscopy, and visual scoring. R.F.-B. extracted RNA and prepared sequencing
562 libraries. M.M. performed the data analyses. M.M and D.C wrote the manuscript.

563

Funding

570 **Conflict of interest**

571 The authors declare that the research was conducted in the absence of any commercial or financial
572 relationships that could be construed as a potential conflict of interest.

573

574 **References**

575 Abe, H., Urao, T., Ito, T., Seki, M., Shinozaki, K., Yamaguchi-Shinozaki, K. (2003). *Arabidopsis*
576 AtMYC2 (bHLH) and AtMYB2 (MYB) function as transcriptional activators in abscisic acid
577 signaling. *Plant Cell*. 15(1), 63–78. doi: 10.1105/tpc.006130

578 Amrine, K. C., Blanco-Ulate, B., Riaz, S., Pap, D., Jones, L., Figueroa-Balderas, R., et al. (2015).
579 Comparative transcriptomics of Central Asian *Vitis vinifera* accessions reveals distinct defense
580 strategies against powdery mildew. *Hortic Res*. 2, 15037. doi: 10.1038/hortres.2015.37

581 Bolger, A. M., Lohse, M., Usadel, B. (2014). Trimmomatic: a flexible trimmer for Illumina
582 sequence data. *Bioinformatics*. 30(15), 2114–2120. doi: 10.1093/bioinformatics/btu170

583 Calonnec, A., Cartolaro, P., Poupot, C., Dubourdieu, D., Darriet, P. (2004). Effects of *Uncinula*
584 *necator* on the yield and quality of grapes (*Vitis vinifera*) and wine. *Plant Pathol*. 53, 434–445.
585 doi: 10.1111/j.0032-0862.2004.01016.x

586 Cochetel, N., Minio, A., Massonnet, M., Vondras, A. M., Figueroa-Balderas, R., Cantu, D. (2021).
587 Diploid chromosome-scale assembly of the *Muscadinia rotundifolia* genome supports
588 chromosome fusion and disease resistance gene expansion during *Vitis* and *Muscadinia*
589 divergence. *G3 (Bethesda)*. 11(4), jkab033. doi: 10.1093/g3journal/jkab033

590 Dalbó, M. A., Ye, G. N., Weeden, N. F., Wilcox, W. F., Reisch, B. I. (2001). Marker-assisted
591 selection for powdery mildew resistance in grapes. *J Amer Soc Hort Sci*. 126(1), 83–89. doi:
592 10.21273/JASHS.126.1.83

593   Danecek, P., Auton, A., Abecasis, G., Albers, C. A., Banks, E., DePristo, M. A., et al. (2011). The
594   variant call format and VCFtools. *Bioinformatics*. 27(15), 2156–2158. doi:
595   10.1093/bioinformatics/btr330

596   Dangl, J. L., Horvath, D. M., Staskawicz, B. J. (2013). Pivoting the plant immune system from
597   dissection to deployment. Science. 341(6147), 746–751. doi: 10.1126/science.1236011

598   Dobin, A., Davis, C. A., Schlesinger, F., Drenkow, J., Zaleski, C., Jha, S., et al. (2013). STAR:
599   ultrafast universal RNA-seq aligner. *Bioinformatics*. 29(1), 15–21. doi:
600   10.1093/bioinformatics/bts635

601   Dombrecht, B., Xue, G. P., Sprague, S. J., Kirkegaard, J. A., Ross, J. J., Reid, J. B., et al. (2007).
602   MYC2 differentially modulates diverse jasmonate-dependent functions in *Arabidopsis*. *Plant Cell*.
603   19(7), 2225–2245. doi: 10.1105/tpc.106.048017

604   Dry, I., Riaz, S., Fuchs, M., Sosnowski, M., Thomas, M. (2019). "Scion breeding for resistance to
605   biotic stresses" in The Grape Genome, ed. D. Cantu, and M. A. Walker (Springer Cham), 319–
606   347. doi: 10.1007/978-3-030-18601-2

607   El-Gebali, S., Mistry, J., Bateman, A., Eddy, S. R., Luciani, A., Potter, S. C., et al. (2019). The
608   Pfam protein families database in 2019. *Nucleic Acids Res*. 47(D1), D427–D432. doi:
609   10.1093/nar/gky995

610   Engström, P. G., Steijger, T., Sipos, B., Grant, G. R., Kahles, A., Rätsch, G., et al. (2013).
611   Systematic evaluation of spliced alignment programs for RNA-seq data. *Nat Methods*. 10(12),
612   1185–1191. doi: 10.1038/nmeth.2722

613   Feechan, A., Anderson, C., Torregrosa, L., Jermakow, A., Mestre, P, Wiedemann-Merdinoglu, S.,
614   et al. (2013). Genetic dissection of a TIR-NB-LRR locus from the wild North American grapevine
615   species *Muscadinia rotundifolia* identifies paralogous genes conferring resistance to major fungal
616   and oomycete pathogens in cultivated grapevine. *Plant J*. 76(4), 661–674. doi: 10.1111/tpj.12327

617   Feechan, A., Kocsis, M., Riaz, S., Zhang, W., Gadoury, D. M., et al. (2015). Strategies for *RUN1*
618   deployment using *RUN2* and *REN2* to manage grapevine powdery mildew informed by studies of
619   race specificity. *Phytopathology*. 105(8), 1104–1113. doi: 10.1094/PHYTO-09-14-0244-R

620   Fung, R. W., Gonzalo, M., Fekete, C., Kovacs, L. G., He, Y., Marsh, E., et al. (2008). Powdery
621   mildew induces defense-oriented reprogramming of the transcriptome in a susceptible but not in a
622   resistant grapevine. *Plant Physiol*. 146(1), 236–249. doi: 10.1104/pp.107.108712

623   Gautam, J. K., Giri, M. K., Singh, D., Chattopadhyay, S., Nandi, A. K. (2021). MYC2 influences
624   salicylic acid biosynthesis and defense against bacterial pathogens in *Arabidopsis thaliana*.
625   *Physiol Plant*. 173(4), 2248–2261. doi: 10.1111/ppl.13575

626   Grabherr, M. G., Haas, B. J., Yassour, M., Levin, J. Z., Thompson, D. A., Amit, I., et al. (2011).
627   Full-length transcriptome assembly from RNA-Seq data without a reference genome. *Nat*
628   *Biotechnol*. 29(7), 644–652. doi: 10.1038/nbt.1883

629   Huson, D. H., Beier, S., Flade, I., Górska, A., El-Hadidi, M., Mitra, S., et al. (2016). MEGAN
630   Community Edition - Interactive Exploration and Analysis of Large-Scale Microbiome
631   Sequencing Data. *PLoS Comput Biol*. 12(6), e1004957. doi: 10.1371/journal.pcbi.1004957

632   Jaillon, O., Aury, J. M., Noel, B., Policriti, A., Clepet, C., Casagrande, A., et al. (2007). The
633   grapevine genome sequence suggests ancestral hexaploidization in major angiosperm phyla.
634   *Nature*. 449(7161), 463–467. doi: 10.1038/nature06148

635   Jiao, C., Sun, X., Yan, X., Xu, X., Yan, Q., Gao, M., et al. (2021). Grape transcriptome response
636   to powdery mildew infection: comparative transcriptome profiling of Chinese wild grapes provides
637   insights into powdery mildew resistance. *Phytopathology*. 111(11), 2041–2051. doi:
638   10.1094/PHYTO-01-21-0006-R

639   Jones, L., Riaz, S., Morales-Cruz, A., Amrine, K. C., McGuire, B., Gubler, W. D., et al. (2014).
640   Adaptive genomic structural variation in the grape powdery mildew pathogen, *Erysiphe necator*.
641   *BMC Genomics*. 15(1), 1081. doi: 10.1186/1471-2164-15-1081

642   Karn, A., Zou, C., Brooks, S., Fresnedo-Ramírez, J., Gabler, F, Sun, Q., et al. (2021). Discovery
643   of the *REN11* locus from *Vitis aestivalis* for stable resistance to grapevine powdery mildew in a
644   family segregating for several unstable and tissue-specific quantitative resistance loci. *Front Plant*
645   *Sci*. 12, 733899. doi: 10.3389/fpls.2021.733899

646   Langmead, B., and Salzberg, S. L. (2012). Fast gapped-read alignment with Bowtie 2. *Nat*
647   *Methods*. 9(4), 357–359. doi: 10.1038/nmeth.1923

648 Leinhos, G. M. E., Gold, R. E., Düggelin, M., Guggenheim, R. (1997). Development and
649 morphology of *Uncinula necator* following treatment with the fungicides kresoxim-methyl and
650 penconazole. *Mycol Res*.101(9), 1033-1046.

651 Li, W., and Godzik, A. (2006). Cd-hit: a fast program for clustering and comparing large sets of
652 protein or nucleotide sequences. *Bioinformatics*. 22(13), 1658–1659. doi:
653 10.1093/bioinformatics/btl158

654 Liang, Z., Duan, S., Sheng, J., Zhu, S., Ni, X., Shao, J., et al. (2019). Whole-genome resequencing
655 of 472 *Vitis* accessions for grapevine diversity and demographic history analyses. *Nat. Commun*.
656 10(1), 1190. doi: 10.1038/s41467-019-09135-8

657 Lolle, S., Stevens, D., Coaker, G. (2020). Plant NLR-triggered immunity: from receptor activation
658 to downstream signaling. *Curr Opin Immunol*. 62, 99–105. doi: 10.1016/j.coi.2019.12.007

659 Love, M. I., Huber, W., Anders, S. (2014). Moderated estimation of fold change and dispersion
660 for RNA-seq data with DESeq2. *Genome Biol*. 15, 550. doi: 10.1186/s13059-014-0550-8

661 Massonnet, M., Vondras, A. M., Cochetel, N., Riaz, S., Pap, D., Minio, A., et al. (2022).
662 Haplotype-resolved powdery mildew resistance loci reveal the impact of heterozygous structural
663 variation on NLR genes in *Muscadinia rotundifolia*. *G3 (Bethesda)*. 12(8), jkac148. doi:
664 10.1093/g3journal/jkac148.

665 McKenna, A., Hanna, M., Banks, E., Sivachenko, A., Cibulskis, K., Kernytsky, A., et al. (2010).
666 The Genome Analysis Toolkit: a MapReduce framework for analyzing next-generation DNA
667 sequencing data. *Genome Res*. 20(9), 1297–1303. doi: 10.1101/gr.107524.110

668 Michelmore, R. W., Christopoulou, M., Caldwell, K. S. (2013). Impacts of resistance gene
669 genetics, function, and evolution on a durable future. *Annu Rev Phytopathol*. 51, 291–319. doi:
670 10.1146/annurev-phyto-082712-102334

671 Minio, A., Cochetel, N., Massonnet, M., Figueroa-Balderas, R., Cantu, D. (2022). HiFi
672 chromosome-scale diploid assemblies of the grape rootstocks 110R, Kober 5BB, and 101-14 Mgt.
673 *Sci Data*. 9(1), 660. doi: 10.1038/s41597-022-01753-0

674　Paniagua, C., Bilkova, A., Jackson, P., Dabravolski, S., Riber, W., Didi, V., et al. (2017). Dirigent
675　proteins in plants: modulating cell wall metabolism during abiotic and biotic stress exposure. *J*
676　*Exp Bot*. 68(13), 3287–3301. doi: 10.1093/jxb/erx141

677　Pap, D., Riaz, S., Dry, I. B., Jermakow, A., Tenscher, A. C., Cantu, D., et al. (2016). Identification
678　of two novel powdery mildew resistance loci, *Ren6* and *Ren7*, from the wild Chinese grape species
679　*Vitis piasezkii*. *BMC Plant Biol*. 16(1), 170. doi: 10.1186/s12870-016-0855-8

680　Patro, R., Duggal, G., Love, M. I., Irizarry, R. A., Kingsford, C. (2017). Salmon provides fast and
681　bias-aware quantification of transcript expression. *Nat. Methods*. 14(4), 417–419. doi:
682　10.1038/nmeth.4197

683　Qiu, W., Feechan, A., Dry, I. (2015). Current understanding of grapevine defense mechanisms
684　against the biotrophic fungus (*Erysiphe necator*), the causal agent of powdery mildew disease.
685　*Hortic Res*. 2, 15020 (2015). doi: 10.1038/hortres.2015.20

686　Quinlan A. R. (2014). BEDTools: The Swiss-Army Tool for Genome Feature Analysis. *Curr*
687　*Protoc Bioinformatics*. 47, 11.12.1–11.12.34. doi: 10.1002/0471250953.bi1112s47

688　Ramming, D. W., Gabler, F., Smilanick, J., Cadle-Davidson, M., Barba, P., Mahanil, S., et al.
689　(2011). A single dominant locus, ren4, confers rapid non-race-specific resistance to grapevine
690　powdery mildew. *Phytopathology*. 101(4), 502–508. doi: 10.1094/PHYTO-09-10-0237

691　Riaz, S., Tenscher, A. C., Ramming, D. W., Walker, M. A. (2011). Using a limited mapping
692　strategy to identify major QTLs for resistance to grapevine powdery mildew (*Erysiphe necator*)
693　and their use in marker-assisted breeding. *Theor Appl Genet*. 122, 1059–1073. doi:
694　10.1007/s00122-010-1511-6

695　Riaz, S., Lejkina, I., Gubler, W., Walker, M. A. (2013). Report of a new grape powdery mildew
696　morphotype with branched conidiophores. *Plant Pathol Quar*. 3, 19–27.

697　Soneson, C., Love, M. I., Robinson, M. D. (2015). Differential analyses for RNA-seq: transcript-
698　level estimates improve gene-level inferences. *F1000Res*. 4, 1521. doi:
699　10.12688/f1000research.7563.2

700 Staswick, P. E., and Tiryaki, I. (2004). The oxylipin signal jasmonic acid is activated by an enzyme
701 that conjugates it to isoleucine in *Arabidopsis*. *Plant Cell*. 16(8), 2117–2127. doi:
702 10.1105/tpc.104.023549

703 Stummer, B.E., Francis, I.L., Zanker, T., Lattey, K.A., Scott, E.S. (2005) Effects of powdery
704 mildew on the sensory properties and composition of Chardonnay juice and wine when grape sugar
705 ripeness is standardised. *Aust J Grape Wine Res*. 11, 66–76. doi: 10.1111/j.1755-
706 0238.2005.tb00280.x

707 Trapnell, C., Williams, B. A., Pertea, G., Mortazavi, A., Kwan, G., van Baren, M. J., et al. (2010).
708 Transcript assembly and quantification by RNA-Seq reveals unannotated transcripts and isoform
709 switching during cell differentiation. *Nat Biotechnol*. 28(5), 511–515. doi: 10.1038/nbt.1621

710 Weng, K., Li, Z. Q., Liu, R. Q., Wang, L., Wang, Y. J., Xu, Y. (2014). Transcriptome of *Erysiphe*
711 *necator*-infected *Vitis pseudoreticulata* leaves provides insight into grapevine resistance to
712 powdery mildew. *Hortic Res*. 1, 14049. doi: 10.1038/hortres.2014.49

713 Yu, Y., Jiao, L., Fu, S., Yin, L., Zhang, Y., Lu, J. (2016). Callose synthase family genes involved
714 in the grapevine defense response to downy mildew disease. *Phytopathology*. 106(1), 56–64. doi:
715 10.1094/PHYTO-07-15-0166-R

716 Zhang, G., Yan, X., Zhang, S., Zhu, Y., Zhang, X., Qiao, H., van Nocker, S., Li, Z., & Wang, X.
717 (2019). The jasmonate-ZIM domain gene *VqJAZ4* from the Chinese wild grape *Vitis*
718 *quinquangularis* improves resistance to powdery mildew in Arabidopsis thaliana. *Plant Physiol*
719 *Biochem*. 143, 329–339. doi: 10.1016/j.plaphy.2019.09.018

720 Zhou, Y., Minio, A., Massonnet, M., Solares, E., Lv, Y., Beridze, T., et al. (2019). The population
721 genetics of structural variants in grapevine domestication. *Nat Plants*. 5(9), 965–979. doi:
722 10.1038/s41477-019-0507-8

723 Zyprian, E., Ochßner, I., Schwander, F., Šimon, S., Hausmann, L., Bonow-Rex, M., et al. (2016).
724 Quantitative trait loci affecting pathogen resistance and ripening of grapevines. *Mol Genet*
725 *Genomics*. 291(4), 1573–1594. doi: 10.1007/s00438-016-1200-5